View metadata, citation and similar papers at core.ac.uk

brought to you by CORE

provided by NASA Technical Reports Server

[redacted]

Copy
RM L55E06

NACA RM L55E06

9791

TECH LIBRARY KAFB, NM
01413

NACA

RESEARCH MEMORANDUM

AN INVESTIGATION OF JET EFFECTS ON ADJACENT SURFACES

By Walter E. Bressette and Maxime A. Faget

Langley Aeronautical Laboratory
Langley Field, Va.

Classification cancelled (or changed to) Unclassified

By Authority of Navy Tech Pub Announcement No 5
(OFFICER AUTHORIZED TO CHANGE)

By [redacted] 22 May 57
NAME AND

[redacted]
GRADE OF OFFICER MAKING CHANGE)

3 Apr 61
DATE

[redacted]

NATIONAL ADVISORY COMMITTEE
FOR AERONAUTICS

WASHINGTON
June 28, 1955

[redacted]

TECH LIBRARY KAFB, NM
0144123

NATIONAL ADVISORY COMMITTEE FOR AERONAUTICS

RESEARCH MEMORANDUM

AN INVESTIGATION OF JET EFFECTS ON ADJACENT SURFACES

By Walter E. Bressette and Maxime A. Faget

SUMMARY

The steady pressure loads as well as the temperature change on adjacent surfaces due to the presence of a propulsive jet at subsonic speeds is shown to be insignificant. Whereas at supersonic speeds the temperature effect might be expected to remain insignificant, the steady pressure loads were shown to increase greatly on surfaces downstream of the propulsive jet exit.

INTRODUCTION

In the past few years an investigation has taken place in the preflight blowdown tunnel at the Langley Aeronautical Laboratory to determine the jet effects on surfaces located in the near vicinity and downstream of a propulsive jet exit. The purpose of this paper is to supplement information already published at Mach number 2.00 with information obtained at other Mach numbers. The jet effects discussed are the steady pressure loads produced on a flat-plate wing due to the presence of a propulsive jet, the heating of the wing surface by the propulsive jet, and the fluctuating pressure frequency spectra superimposed on the wing steady pressures from the propulsive jet.

SYMBOLS

D_j	diameter of sonic exit
D_{j_*}	diameter of sonic throat
ΔC_N	incremental normal-force coefficient, $\frac{\Delta N_{total}}{qS_{j_*}}$
H_j	total pressure at exit of nacelle
M_o	free-stream Mach number

[redacted]

NAB055 3094S

ΔN	incremental normal force, $(\text{Normal force})_{\text{jet on}} - (\text{Normal force})_{\text{jet off}}$
P	wing pressure coefficient, $\frac{p_w - p_o}{q}$
ΔP	incremental pressure coefficient, $P_{\text{jet on}} - P_{\text{jet off}}$
p_w	wing static pressure
p_o	free-stream static pressure
$\bar{p}$	overall acoustic pressure fluctuations
q	free-stream dynamic pressure
S_{j_*}	area of sonic throat
T_{WING}	static temperature on wing
T_{s_o}	free-stream stagnation temperature
V_e	velocity at the nacelle exit
x	chordwise distance on wing from nacelle exit (downstream positive)
y	spanwise distance on wing from nacelle center line

APPARATUS

Presented in figure 1 is a three-dimensional sketch of the test setup showing a small-scale nacelle mounted below a flat-plate wing at the exit of the preflight blowdown tunnel. The general airplane configurations in the figure are the type of airplane configurations that this test setup would apply to. The shaded areas on the configurations are the areas most likely to experience the type of jet effects that are discussed in this paper.

Presented in figure 2 is a side view of the test setup showing the small-scale nacelle, having a 5° boattail angle, mounted at $3.35D_j$ below the flat-plate wing at the exit of the preflight blowdown tunnel. Although more than one vertical position was tested in this investigation,

a vertical position of $3.35D_j$ was selected for this paper in order to correlate the additional data with an exact position that has already been published at a Mach number of 2.00 (ref. 1). The nacelle at this position was tested with two types of exit nozzles, a convergent nozzle called a sonic exit and a convergent-divergent nozzle called a supersonic exit, both having the same size sonic throat.

INSTRUMENTATION

Figure 3 shows the location from the nacelle exit of 47 static-pressure orifices on the wing as well as the high-frequency pressure pickup and a thermocouple plate with 24 thermocouples that was installed in a similar wing.

RESULTS AND DISCUSSION

The pressure field on the wing with nacelle jet off is presented in figure 4 and shows the nacelle wake which is responsible for the formation in the free-stream flow of a jet-off trailing wake shock wave. In the jet-off operation, the pressure is negative downstream of the nacelle exit because of the presence of the nacelle boattail angle and rises to a positive pressure further downstream because of the intersection on the flat-plate wing of the jet-off trailing wake shock wave.

In figure 5 is presented a typical nacelle jet-on pressure field on the wing showing the propulsive jet issuing from the exit of the nacelle and flowing downstream below the flat-plate wing. In the jet-on operation, a shock wave (called the primary shock wave) forms at the exit of the nacelle, and the impingement on the wing of this shock wave is responsible for the formation of the first positive pressure in the field. This positive pressure gradually falls off in pressure until a second positive pressure rise occurs, which is less intense than the first one. This second positive pressure rise is caused by the intersection on the wing of a second jet-on shock wave (called the secondary shock wave) that is formed in the propulsive jet wake downstream of the nacelle exit.

Presented in figure 6 is the axial pressure distribution downstream of the nacelle exit for both jet on and jet off at the same value of H_j/p_o for M_o of 1.40, 1.80, and 2.00. The first positive pressure rise on the wing with jet on moves farther to the rear of the nacelle exit with an increase in M_o. This effect is the result of decreasing the primary shock-wave angle when M_o is increased at a constant value of H_j/p_o.

[redacted]

NACA RM L55E06 30948

Because all pressures on the wing vary with nacelle-exit jet off depending upon the general configuration of the nacelle, the pressure on the wing also varies with the nacelle jet on; but the increment of pressure between jet on and jet off, or the pressure on the wing due to the presence of the propulsive jet, should remain the same. Therefore, all discussion of pressures and loads that follow in this paper will be in the form of incremental pressures and incremental loads.

Shown in figure 7 is the incremental pressure field due to the nacelle jet wake for a sonic exit and a supersonic exit at the same H_j/p_o.

When jet-on and jet-off wing pressure data were combined to form the incremental pressure data, positive incremental pressure resulted immediately behind the intersection on the wing of the primary shock wave. This positive incremental pressure gradually decreased until it became negative in the vicinity of the intersection on the wing of the jet-off trailing wake shock and it remained negative to the end of the wing.

The primary shock-wave angle was lower in angle for the supersonic exit than it was for the sonic exit. Therefore, the positive pressure behind the shock wave as well as the area upon which it acts was reduced.

From an integration of these chordwise incremental pressure profiles, the spanwise incremental wing loading can be obtained. In figure 8 the relative spanwise incremental wing loading is presented for a sonic exit with $H_j/p_o = 6$ for M_o of 1.40, 1.80, and 2.00.

With an increase in M_o, the spanwise distance from the nacelle-exit center line upon which the loads act is decreased. This is a result of decreasing the primary shock-wave angle by increasing M_o. Also shown is a subsonic test made at $M_o = 0.80$ and $H_j/p_o = 3.37$. From this test, slight negative pressures on the wing were obtained. From an integration of the spanwise wing loading, ΔC_N can be obtained.

Figure 9 presents the variation of ΔC_N with H_j/p_o for a nacelle sonic exit at M_o of 1.40, 1.80, 2.00, and 0.80. The value of ΔC_N at a constant value of H_j/p_o in the supersonic range is decreased with an increase in M_o; but with the ΔC_N curves tending to increase with an increase in H_j/p_o and with present-day turbojet engines indicating that a maximum value of H_j/p_o of 5 will be produced at $M_o = 1.40$, of 9 at $M_o = 1.80$, and of 10 at $M_o = 2.00$, then a nearly constant ΔC_N is indicated from this flat-plate-wing analysis for maximum cruising operation.

In figure 10 is presented the variation of ΔC_N with H_j/p_o for a nacelle sonic exit and a nacelle supersonic exit at $M_o = 1.40$. The value of ΔC_N was reduced at all H_j/p_o tested by using a nacelle supersonic exit.

Presented in figure 11 is the variation of the ratio of ΔN to thrust with H_j/p_o for a nacelle sonic exit at all free-stream supersonic Mach numbers tested. As can be seen in the figure there is little difference in the ratio of ΔN to thrust with a decrease in M_o, and a mean lower value of 0.6 was obtained at a nacelle-exit pressure ratio of 7. Although ΔN increased with an increase in H_j/p_o, this figure shows that it did not increase as rapidly as the thrust did.

In figure 12 is presented the axial temperature distribution downstream of the nacelle exit at $M_o = 0.80$ with nacelle jet on and nacelle jet off. The ordinate of the curves is the ratio of the temperature as measured on the wing during steady-state conditions divided by the free-stream stagnation temperature. A nacelle jet temperature of 1,500° F with $H_j/p_o = 4$ was obtained for the jet-on tests by burning hydrogen in air at a low fuel-air ratio. The broken lines show the temperature distribution with nacelle jet off. The solid lines show the temperature distribution with the nacelle jet on at two vertical positions from the wing, the higher one being at $1.7D_j$ from the wing and the lower one being at $3.35D_j$ from the wing. The maximum difference between jet-off temperature and jet-on temperature is less than 10° F indicating very little heating due to the presence of the propulsive jet. It should be noted that the hot exhaust gas in the propulsive jet wake did not penetrate the free-stream flow to the wing surface in a distance of $6D_j$ downstream of the nacelle exit.

Presented in figure 13 is the frequency spectra of $\bar{p}$ that were obtained at a point immediately behind the intersection on the wing of the primary shock wave, whereas H_j/p_o was varied from 7 to 2 at $M_o = 1.80$ for a nacelle sonic exit and a nacelle supersonic exit. These data were preliminary and were obtained with a specially designed pickup using a small-scale nacelle having a sonic throat of 0.72 inch in diameter. These data show that $\bar{p}$ is greater for the supersonic exit than it was for the sonic exit. Also, the range of pressures is essentially in agreement with that obtained by Lassiter and Hubbard (ref. 2), for a sonic jet with no free-stream flow.

CONCLUDING REMARKS

The steady pressure loads as well as the temperature change on adjacent surfaces due to the presence of a propulsive jet at subsonic speeds is shown to be insignificant. Whereas at supersonic speeds the temperature effect might be expected to remain insignificant, the steady pressure loads were shown to increase greatly on surfaces downstream of the propulsive jet exit.

Langley Aeronautical Laboratory,
National Advisory Committee for Aeronautics,
Langley Field, Va., April 20, 1955.

REFERENCES

1. Bressette, Walter E.: Investigation of the Jet Effects on a Flat Surface Downstream of the Exit of a Simulated Turbojet Nacelle at a Free-Stream Mach Number of 2.02. NACA RM L54E05a, 1954.

2. Lassiter, Leslie W., and Hubbard, Harvey H.: The Near Noise Field of Static Jets and Some Model Studies of Devices for Noise Reduction. NACA TN 3187, 1954.

APPLICATION OF JET EFFECTS

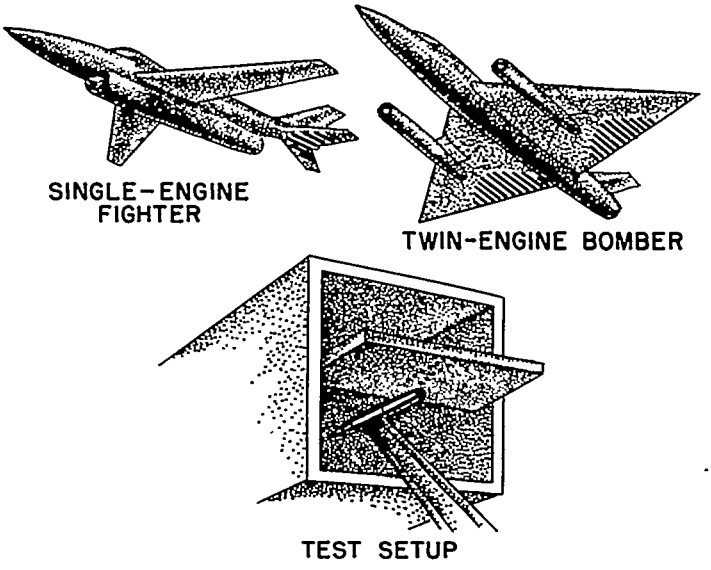

Figure 1

TEST SETUP
(SIDE VIEW)

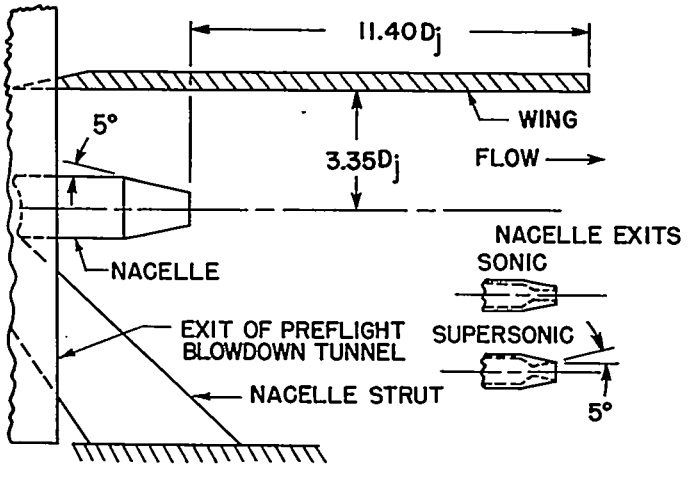

Figure 2

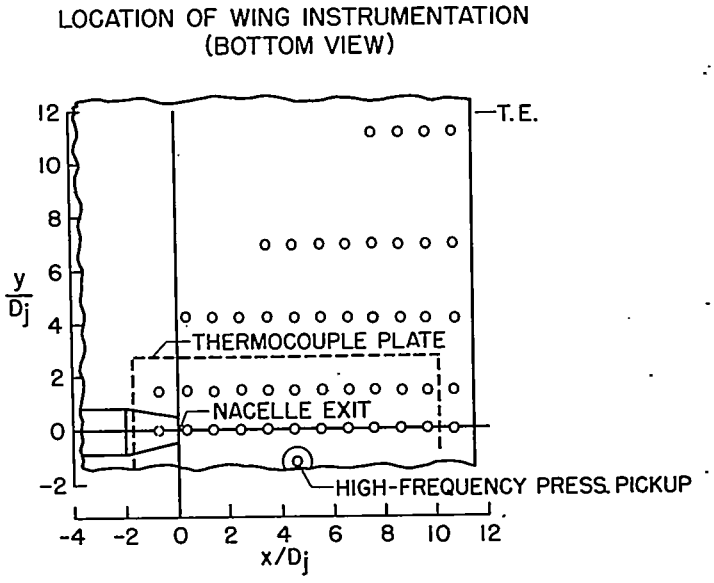

Figure 3

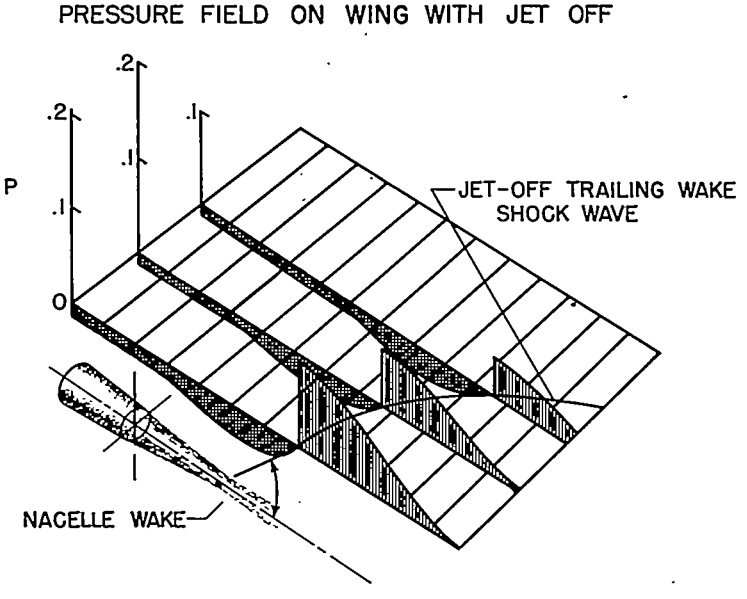

Figure 4

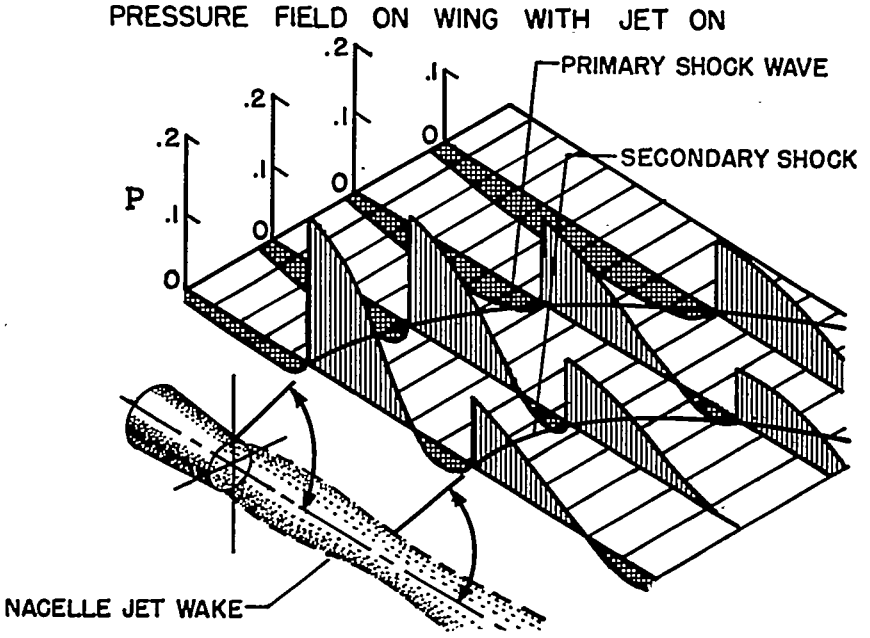

Figure 5

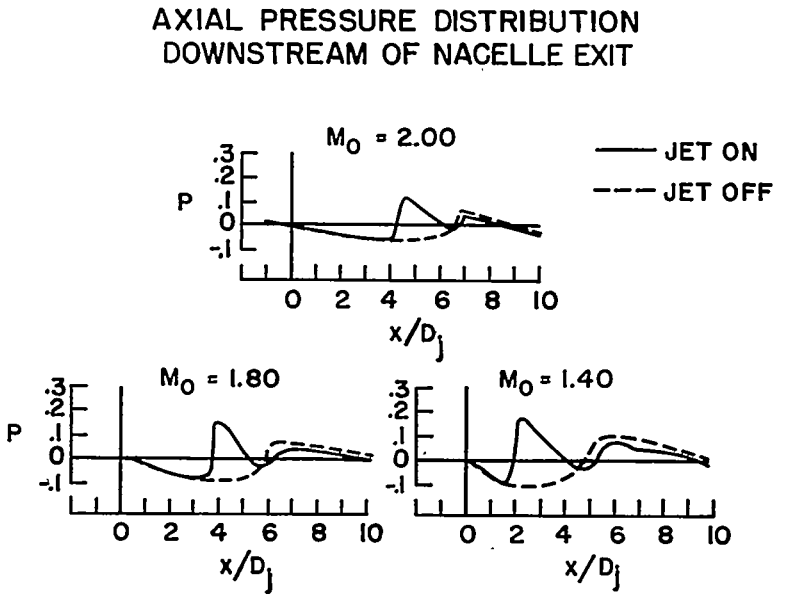

Figure 6

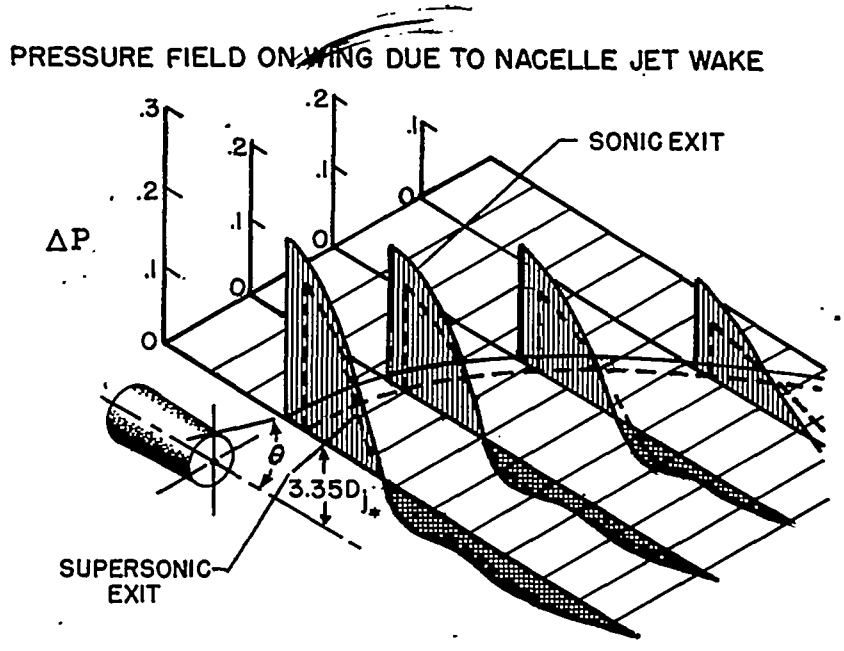

Figure 7

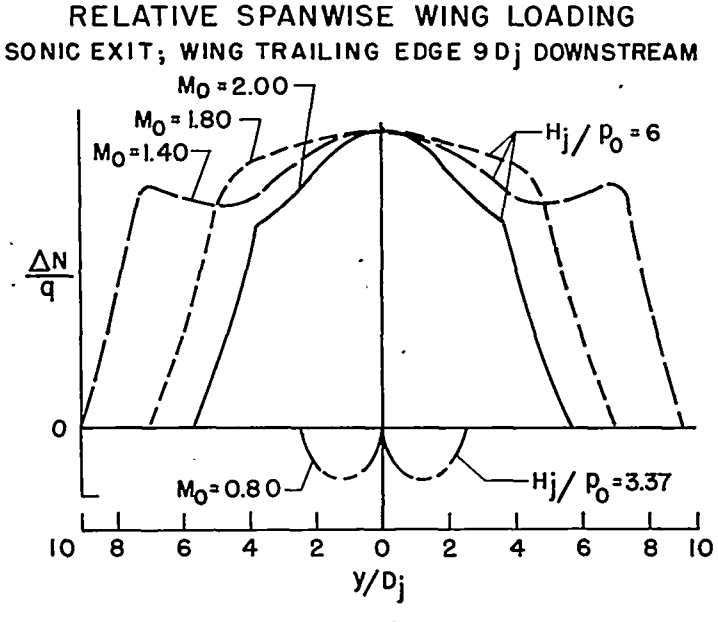

Figure 8

VARIATION OF NORMAL-FORCE COEFFICIENT
SONIC EXIT; WING TRAILING EDGE $9D_j$ DOWNSTREAM

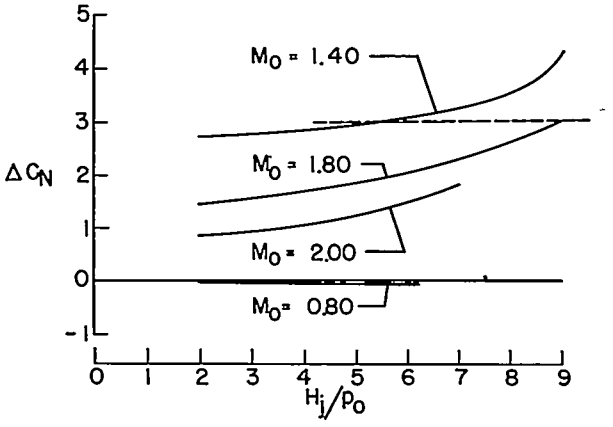

Figure 9

NORMAL-FORCE COEFFICIENT FOR
SONIC AND SUPERSONIC NACELLE EXITS
M_0=1.40

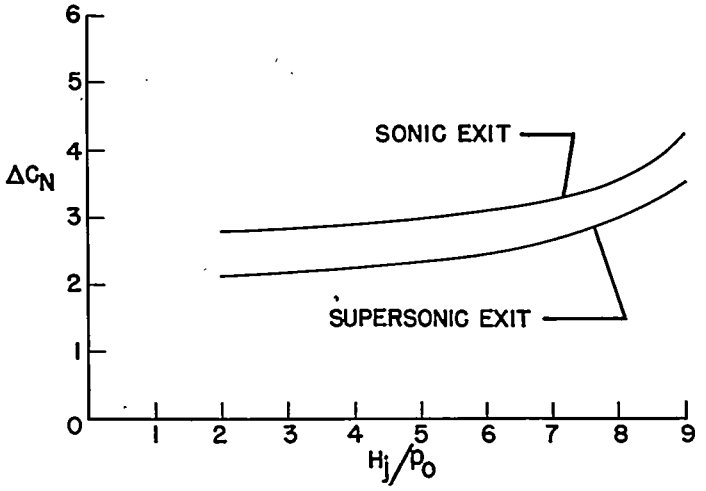

Figure 10

[redacted]

VARIATION OF RATIO OF NORMAL FORCE TO THRUST WITH PRESSURE RATIO
SONIC EXIT

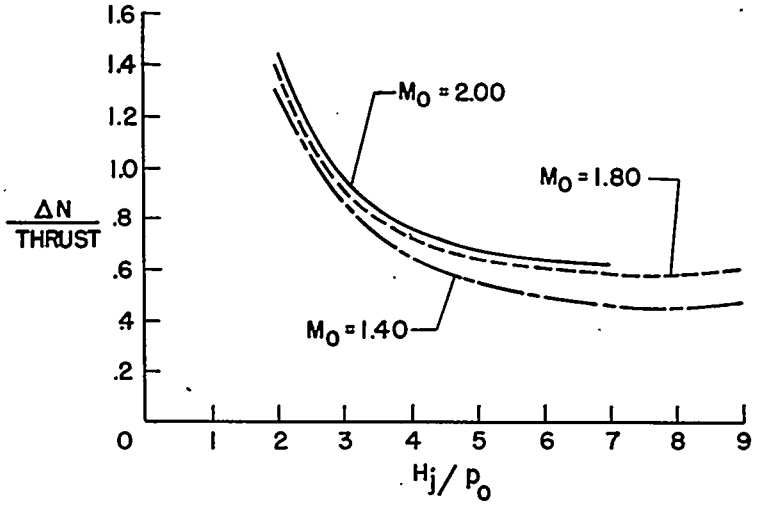

Figure 11

AXIAL TEMPERATURE DISTRIBUTION DOWNSTREAM OF NACELLE EXIT
M_0 = 0.80; JET TEMPERATURE, 1500° F; H_j/p_0 = 4

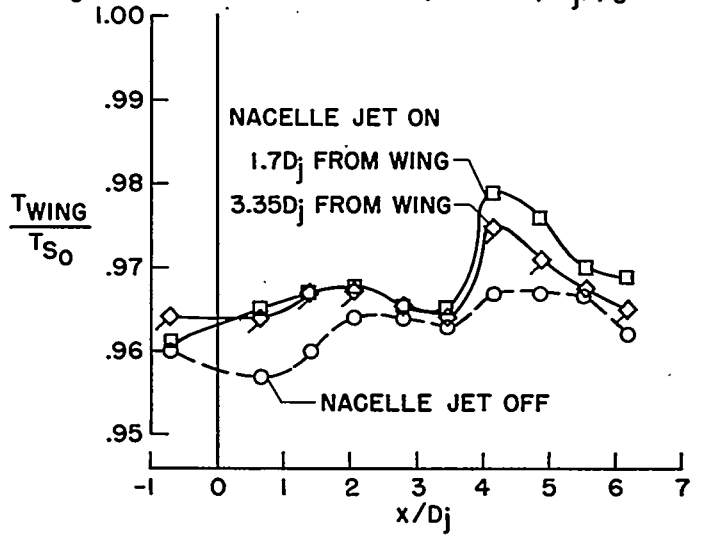

Figure 12

[redacted]

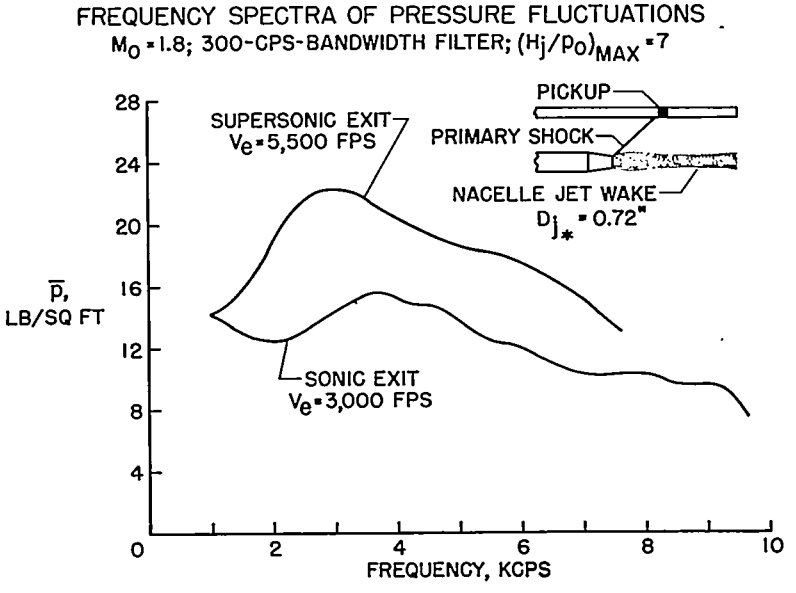
FREQUENCY SPECTRA OF PRESSURE FLUCTUATIONS
M_0 = 1.8; 300-CPS-BANDWIDTH FILTER; $(H_j/P_0)_{MAX}$ = 7
PICKUP
SUPERSONIC EXIT
V_e = 5,500 FPS
PRIMARY SHOCK
NACELLE JET WAKE
D_{j_*} = 0.72"
SONIC EXIT
V_e = 3,000 FPS
$\overline{p}$, LB/SQ FT
28
24
20
16
12
8
4
0
2
4
6
8
10
FREQUENCY, KCPS

Figure 13